THE JOURNAL OF BIOLOGICAL CHEMISTRY
Vol. 279, No. 31, Issue of July 30, pp. 32367–32372, 2004

Printed in U.S.A.

Weak Base Permeability Characteristics Influence the Intracellular Sequestration Site in the Multidrug-resistant Human Leukemic Cell Line HL-60*[S]

Received for publication, January 22, 2004, and in revised form, May 19, 2004
Published, JBC Papers in Press, June 3, 2004, DOI 10.1074/jbc.M400735200

Muralikrishna Duvvuri, Yuping Gong, Dev Chatterji, and Jeffrey P. Krise‡

From the Division of Drug Delivery and Disposition, School of Pharmacy, University of North Carolina at Chapel Hill, Chapel Hill, North Carolina 27599

A number of organelles contained within mammalian cells have been implicated in the selective sequestration of chemical entities including drug molecules. Specifically, weakly basic molecules have been shown to selectively associate with either the mitochondrial compartment or lysosomes; however, the structural basis for this differentiation has not been understood. To investigate this, we have identified a series of seven weakly basic compounds, all with pK_a near neutrality, which have different sequestration sites within the multidrug-resistant HL-60 human leukemic cell line. Three of the compounds were selectively sequestered into the mitochondria of the cells, whereas the remainder were predominantly localized within lysosomes. Using specific chemical inhibitors to disrupt either mitochondrial or lysosomal accumulation capacity, we demonstrated that accumulation of these compounds into respective organelles are not competitive processes. Comparison of the permeability characteristics of these compounds as a function of pH revealed striking differences that correlate with the intracellular sequestration site. Only those compounds with significantly reduced permeability in the ionized state relative to the un-ionized state had the capacity to accumulate within lysosomes. Alternatively, those compounds with relatively pH-insensitive permeability selectively accumulated into mitochondria. Using novel quantitative assays for assaying drug accumulation into subcellular organelles, we demonstrated a correlation between these permeability characteristics and the lysosomal *versus* mitochondrial accumulation capacity of these compounds. Together, these results suggest that the selective accumulations of weakly basic compounds in either lysosomes and mitochondria occur via exclusive pathways governed by a unique permeability parameter.

The development of the multidrug-resistant (MDR)[1] phenotype in cancer cells is associated with a variety of physiological and biochemical changes (1, 2). Our laboratory investigated the intracellular drug sequestration pathways associated with the emergence of this drug-resistant phenotype. We have recently shown that selective accumulation of anticancer drugs in cellular organelles of the MDR human leukemic cell line HL-60 can be associated with decreased drug effectiveness (3). Moreover, we also have shown that different organelles are able to sequester drugs with different structural attributes according to independent mechanisms. A remaining paradox in this field of research has to do with the intracellular sequestration site of weakly basic compounds. We along with others have shown that certain weakly basic compounds (*i.e.* daunorubicin, doxorubicin) with pK_a values near neutrality are selectively sequestered into lysosomes of MDR cell lines (3, 4). Alternatively, other weakly basic compounds, also with pK_a near neutrality, specifically accumulate within the mitochondria of cells (*i.e.* rhodamine 123) (5). Independent theories have been put forth to describe weak base sequestration into each of these compartments; however, a physicochemical parameter that can be used to predict the intracellular sequestration site has not been elucidated.

Selective accumulation of weakly basic drugs into the lysosomal compartment of MDR cells is thought to occur according to a pH partitioning type of mechanism that relies on the low pH of lysosomes relative to the cell cytosol (6–8). In the MDR HL-60 cell line, we have previously determined that the pH values associated with the lysosomal lumen and cell cytosol are 5.2 and 7.1, respectively (3). Following permeation through the cell membrane, weakly basic drugs with pK_a near neutrality would exist to a significant degree in their un-ionized membrane-permeable form in the cytosol. In this form, they are able to diffuse through the lysosomal lipid bilayer and enter the lumen. Here in the acidic environment, the base would exist predominantly in the ionized form. Because ionized forms of drugs are traditionally thought to be membrane impermeable, the weak base becomes trapped within the lysosome, which can lead to significant accumulation as long as the pH gradient is maintained.

The accumulation mechanism for weak bases into the mitochondrial compartment is driven by the negative membrane potential associated with this organelle. The mitochondrial transmembrane proton motive force, which is generated by oxidative phosphorylation, results in both a pH differential (more alkaline inside) and an electrical potential (more negative inside) (9). This membrane potential difference has been estimated to be −150 to −170 mV and can result in the accumulation of cationic molecules several hundred-fold over cytoplasmic concentrations (10).

The site of intracellular sequestration of weakly basic compounds is an important consideration for effective drug target-

* The costs of publication of this article were defrayed in part by the payment of page charges. This article must therefore be hereby marked "*advertisement*" in accordance with 18 U.S.C. Section 1734 solely to indicate this fact.

[S] The on-line version of this article (available at http://www.jbc.org) contains supplemental Figs. 6–9.

‡ To whom correspondence should be addressed: Dept. of Pharmaceutical Chemistry, University of Kansas, Lawrence, KS 66045. Tel.: 785-864-4822; E-mail: krise@ku.edu.

[1] The abbreviations used are: MDR, multidrug-resistant; QNC, quinacrine; DNP, 2,4-dinitrophenol; HAR, harmine; PAP, papaverine; NF, New Fuchsin; LTR, Lysotracker Red DND-99; R123, rhodamine 123; R6G, rhodamine 6G; PBS, phosphate-buffered saline; FeDex, iron dextran; HPLC, high pressure liquid chromatography; TRITC, tetramethylrhodamine isothiocyanate.

ing. Drug targets are typically housed within specific cellular compartments, and the ability of a drug to accumulate therein has a bearing on drug activity and specificity. The quest to specifically target novel anticancer agents to the mitochondrial compartment has received much recent interest and many lipophilic cationic molecules have been evaluated as anticancer agents (11). Significant accumulation of such compounds into the mitochondria has varied effects; nevertheless, the end result is often diminished cellular ATP production, which in turn triggers cell death (11). From a drug delivery point of view, the attractiveness of this therapeutic approach is centered on the finding that cancer cells have increased negative membrane potential relative to nontransformed cells (11). This difference is expected to result in a 10-fold higher concentration in the mitochondria of cancer cells than those of nontransformed cells. Unfortunately, the design of mitochondrially targeted, weakly basic anticancer drugs has been complicated by the fact that many of these agents are sequestered by lysosomes, which diminishes the aforementioned specificity. Furthermore, the effectiveness of many traditional weakly basic anticancer agents is also lessened as a result of lysosomal sequestration in MDR cancer cells. Many of these agents (*i.e.* daunorubicin, doxorubicin) have nuclear targets including DNA and topoisomerase (12). Consequently, lysosomal sequestration results in reduced interactions with targets and decreased effectiveness. Taken together, drug design efforts would greatly benefit from an understanding of physicochemical parameters that predictably influence intracellular localization.

To address this paradox we have evaluated the physicochemical properties of a series of weakly basic compounds that are preferentially sequestered into lysosomes or mitochondria. We report here that the permeability of the ionized species relative to un-ionized species is a principal determinant of subcellular distribution.

EXPERIMENTAL PROCEDURES

The doxorubicin-selected resistant human acute promyeloid leukemia cell line MDR HL-60 was kindly provided by Dr. Yueshang Zhang (Arizona Cancer Center, University of Arizona). MDR HL-60 cells were grown in RPMI 1640 medium supplemented with 10% fetal calf serum, 10 mM Hepes, 1 mM sodium pyruvate, 0.1% penicillin, and 0.1% streptomycin. The cells were maintained at a density of 1×10^5 to 1×10^6 cells/ml at 37 °C in a humidified 5% CO_2 atmosphere. Quinacrine (QNC) and 2,4-dinitrophenol (DNP) were kindly provided by Dr. Moo Cho (School of Pharmacy, University of North Carolina-Chapel Hill). Harmine (HAR), papaverine (PAP), New Fuchsin (NF), 1-octanol and concanamycin A (Con A) were purchased from Sigma. Lysotracker Red DND-99 (LTR), rhodamine 123 (R123), and rhodamine 6G (R6G) were obtained from Molecular Probes (Eugene, OR).

Fluorescence Microscopy—Cells were grown to a density of 1×10^6 cells/ml prior to experimentation. The cells were incubated with the indicated compound (1 μM) for 2 h under normal growth conditions. Following incubation, the cells were pelleted (1000 rpm, 5 min) and washed twice with ice-cold PBS to remove any unincorporated compound. Disruption of lysosome-to-cytosol pH gradient was achieved with a 24-h pre-incubation with 20 nM Con A. Disruption of mitochondrial membrane potential was achieved with a 30-min pre-incubation of cells with 100 μM DNP. The cells were viewed with a microscope (Leica Diaplan, Leitz Weltzar, Germany) equipped for epifluorescence with a 100× objective, and images were captured using an Orca ER camera (Hamamatsu Corp.) controlled by SimplePCI imaging software (Compix Inc.). R6G and LTR utilized a Texas Red filter set, whereas a fluorescein filter set was employed for QNC and R123.

pH Partition Experiments—The pH partition behavior of each test compound was evaluated in *n*-octanol/buffer systems using the shake-flask method (13). Briefly, the test compounds were dissolved to a final concentration of 1 μM in 10 ml of an aqueous solution containing 5 mM Hepes, 5 mM ammonium acetate, 5 mM KCl, and 154 mM NaCl (300 mosM; pH 4–11 adjusted with 0.1 N NaOH or 0.1 N HCl). 1-octanol (0.5–1.0 ml) was added, and the two-phase system was shaken (150 oscillations/min) for 30 min at 25 °C. The phases were separated by centrifugation at 3000 rpm for 10 min. Aliquots (10–100 μl) of each phase were appropriately diluted and assayed for compound using a PerkinElmer Life Sciences LS50B spectrofluorometer. Intrinsic partition coefficients of ionized (PC_i) and un-ionized base (PC_u) were obtained by curve fitting the pH partition profiles for QNC, LTR, HAR, and PAP using SigmaPlot 2001 (SPSS Inc., Chicago, IL) using the Hill equation (4 parameters). For NF, R123, and R6G, PC_i and PC_u were estimated as partition coefficients at pH values 3 units below and above the pK_a, respectively. The ratio of PC_i to PC_u was defined as the α value. Log *p* values for test compounds were obtained by taking the common logarithm of the corresponding PC_u.

pK_a Determinations—The pK_a values for QNC, LTR, HAR, and PAP were obtained by curve fitting the respective pH partition profiles as described under "pH Partition Experiments." The pK_a values for the rhodamine derivatives were obtained by monitoring the change in fluorescence emission as a function of pH. Buffer composition was identical to that used for pH partition experiments. Fluorescence measurements were made using a PerkinElmer Life Sciences LS50B spectrofluorometer. The excitation and emission wavelengths used for R123 were $\lambda_{Ex} = 508$ and $\lambda_{Em} = 525$ nm and for R6G, $\lambda_{Ex} = 528$ and $\lambda_{Em} = 551$ nm. The pH *versus* fluorescence emission profiles were modeled using SigmaPlot 2001 with the Hill equation (4 parameters), and the pK_a value was obtained. The pK_a value for NF was obtained by monitoring the change in absorbance at 542 nm as a function of pH. Buffer composition was identical to that used for pH partition experiments. Absorbance measurements were made using a Shimadzu UV-2401 PC spectrophotometer. The pH *versus* absorbance profile was modeled using SigmaPlot 2001 with the Hill equation (4 parameters), and the pK_a value was obtained.

Isolation of Lysosomes from MDR HL-60 Cells—Lysosomes were isolated using a magnetic chromatographic approach described by Diettrich *et al.* (14) with modifications. Superparamagnetic iron dextran particles (FeDex) were prepared as described therein. MDR HL-60 cells (200×10^6 cells) were incubated with FeDex particles (2 mg/ml) for 1 h at 37 °C in PBS, pH 7.4, to allow for endocytic uptake. Following the initial 1-h incubation, the cells were washed four times with PBS and incubated in FeDex-free medium at 37 °C for 24 h to allow for the specific lysosomal association of FeDex particles. At the end of the chase, the cells were washed twice with ice-cold PBS and homogenized in 2 ml of hypotonic buffer containing 15 mM potassium chloride, 1.5 mM magnesium acetate, 1 mM dithiothreitol, and 10 mM Hepes (pH 7.4) supplemented with 0.1 mM phenylmethylsulfonyl fluoride, 0.5 mg/ml DNase I, and 1 μg/ml each aprotinin, leupeptin, and pepstatin. The cells were homogenized in a Dounce homogenizer (15 strokes) using the tight fitting pestle (pestle B). To the homogenate was added 0.5 ml of hypertonic buffer containing 375 mM potassium chloride, 22.5 mM magnesium acetate, 1 mM dithiothreitol, and 220 mM Hepes at pH 7.4 and centrifuged at 1750 rpm for 10 min to pellet the nuclei and unbroken cells. The resultant post-nuclear supernatant was passed through a mini-Macs column (Miltenyi Biotec) contained in a magnetic sleeve. The column had been equilibrated previously with 500 μl of 0.5% bovine serum albumin in PBS. Without letting the column go dry, two column volumes of PBS containing 0.5 mg/ml DNase I were allowed to pass through the column and then allowed to stand in the column for 10 min. The column was then washed with 500 μl of ice-cold PBS. The column contents were eluted with PBS containing 0.5% Triton X-100 that was allowed to stand for 10 min prior to removal of the column from the magnet. The eluted fraction was highly enriched in lysosomes without detectable contamination from other cellular organelles. Approximately 29% of the total cellular lysosomes were recovered in this fraction (see Fig. 9 of supplementary data) as evaluated using enzyme assays described by Ford *et al.* (15).

Isolation of Cytosol from MDR HL-60 Cells—Cytosol isolation was carried out according to a procedure described previously by our laboratory (16). Recovery of cytosol in the isolated fraction was 100% based on this method.

Isolation of Mitochondria from MDR HL-60 Cells—A differential centrifugation method was developed to obtain an enriched fraction of mitochondria with minimal lysosomal contamination. Briefly, 2 ml of post-nuclear supernatant was generated from 200×10^6 MDR HL-60 cells as described under "Isolation of Lysosomes from MDR HL-60 Cells." The post-nuclear supernatant was placed on top of a 1 M sucrose layer (2 ml) and centrifuged at 3250 rpm for 15 min. The resultant pellet was enriched in mitochondria without significant contamination from other organelles. This pellet contained ~23% of total cellular mitochondria as evaluated using enzyme assays (Fig. 9 of supplementary data).

Quantitation of Compounds in Cytosol, Mitochondria, and Lysosome Fractions—Cytosol, mitochondria, and lysosomes were isolated from

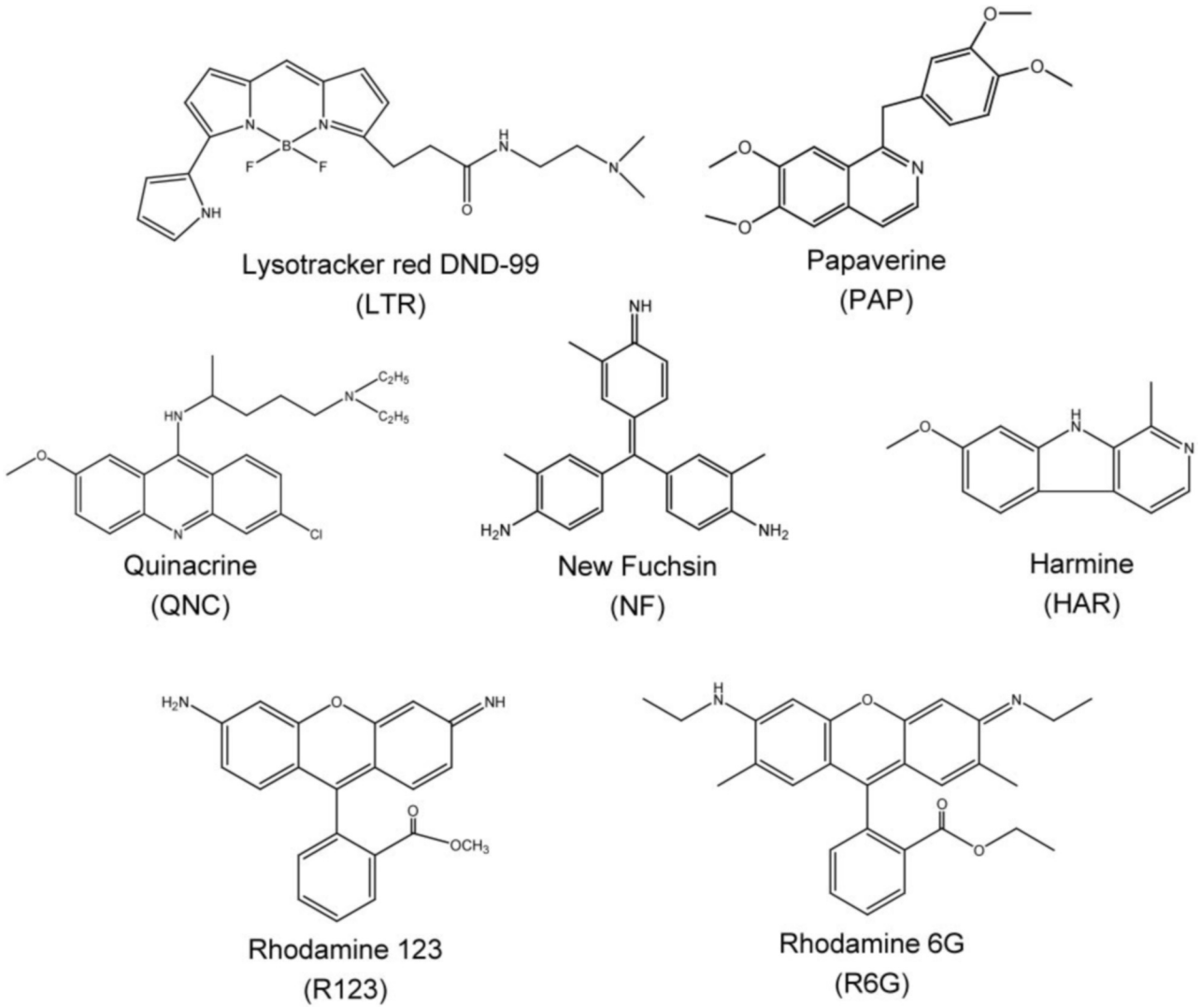

FIG. 1. **Structures of weakly basic compounds evaluated in this study.** QNC and LTR are fluorescent molecules that selectively accumulate within the lysosomes of cells. R123 and R6G are fluorescent molecules that accumulate in the mitochondrial compartments of cells. HAR, PAP, and NF are weak bases with unknown intracellular distribution.

MDR HL-60 cells incubated previously with compound for 12 h. Each of these isolated cellular fractions was vortexed for 30 s with 600 μl of acetonitrile and centrifuged at 13,200 rpm for 5 min. The supernatant was evaporated to dryness, and the residue was dissolved in 100 μl of an appropriate HPLC mobile phase and analyzed. The amount of compound extracted from each isolated cellular fraction was thus quantitated.

Extraction efficiencies of each compound from cytosolic, lysosomal, and mitochondrial fractions were separately determined and incorporated in our calculations. This is done to account for the loss of compound from each isolated cellular fraction during the extraction procedure. Extraction efficiencies and standard curves were determined by spiking known amounts of each test compound (5 different amounts, representing high, medium, and low concentrations) into blank cellular fractions and carrying out the extraction procedure described in the previous paragraph. Standard curves were linear with $r^2 > 0.98$. Extraction efficiencies for all the test compounds ranged from 50 to 95%.

To compare lysosomal accumulation between compounds, the amount of each compound in lysosomes (per cell) was divided by that in cytosol. This value was defined as the extent of lysosomal accumulation. This was done to account for the intrinsic permeability differences between compounds. Similarly, the extent of mitochondrial accumulation for each compound was obtained by dividing the amount of compound in mitochondria (per cell) to that in cytosol. To compare lysosome *versus* mitochondrial accumulation of compounds, the extent of lysosomal accumulation was divided by the extent of mitochondrial accumulation. In all the quantitative calculations, organelle isolation efficiencies (lysosomes, 29%; mitochondria, 23%; and cytosol, 100%) were incorporated.

HPLC Analysis—A Waters 600E system controller, 616 pump, and 717 plus autosampler comprised the HPLC system. A Waters Xterra® MS C_{18} column was used. The mobile phase contained acetonitrile in 10 mM ammonium formate (pH 4.0). The percent composition of acetonitrile in the mobile phase for each compound was as follows: 20% for HAR, 22% for PAP, 25% for QNC and R123, 28% for LTR and NF, and 40% for R6G. In addition, the mobile phase for R6G consisted of 20% methanol. A 474 fluorescence detector (Waters Corp., MA) was used to detect R123, R6G, HAR, LTR, and QNC. The excitation and emission wavelengths for the fluorescent compounds were as follows: HAR (λ_{Ex} = 350 nm; λ_{Em} = 427 nm), QNC (λ_{Ex} = 463 nm; λ_{Em} = 500 nm), R123 (λ_{Ex} = 508 nm; λ_{Em} = 525 nm), LTR (λ_{Ex} = 577 nm; λ_{Em} = 590 nm), and R6G (λ_{Ex} = 528 nm; λ_{Em} = 551 nm). PAP and NF were detected using a Rainin Dynamax absorbance detector (Model UV-C) at 248 nm and 542 nm, respectively.

RESULTS

Model Compound Selection—The determination of relevant physicochemical parameters that influence lysosomal *versus* mitochondrial accumulation was achieved by evaluating a series of seven weakly basic compounds. The structures of these compounds are shown in Fig. 1. R123 and R6G are fluorescent vital stains that have been shown to specifically associate with the mitochondrial compartments of these cells. QNC and LTR are fluorescent compounds that have been shown to specifically accumulate within the lysosomes of cells. To the best of our ability, we selected weakly basic compounds for this evalua-

TABLE I
Physicochemical properties of test compounds

Compound[a]	M_r	pK_a[b]	Log P[b,c]	α[b,c]
QNC	399.9	8.0	1.85 ± 0.03	0.004 ± 0.001
PAP	339.3	7.3	2.68 ± 0.11	0.006 ± 0.001
LTR	399.2	7.5	2.10 ± 0.02	0.017 ± 0.001
HAR	212.2	7.7	2.20 ± 0.06	0.023 ± 0.004
NF	329.4	6.9	1.96 ± 0.03	0.72 ± 0.07
R123	380.8	7.2	1.06 ± 0.06	1.004 ± 0.090
R6G	479.0	7.5	2.37 ± 0.02	1.440 ± 0.220

[a] For structure see Fig. 1.
[b] Experimentally determined values.
[c] Values are means of three determinations ± S.D.

tion, which had comparable pK_a values that are near neutrality. This is an important consideration, because the pK_a of the weak base would be expected to predictably influence both lysosomal and mitochondrial accumulation behavior. The experimentally determined pK_a values for each of these compounds are shown in Table I. In addition to the above compounds, we selected the weak bases HAR, PAP, and NF, all of which had pK_a values near neutrality; however, their intracellular distribution profiles were unknown.

Evaluation of Sequestration Sites and Mechanisms—The fact that QNC, LTR, R123, and R6G (Fig. 1) are fluorescent allowed us to characterize their intracellular distribution using fluorescence microscopy. MDR HL-60 cells incubated with these compounds displayed distinct punctate intracellular accumulation patterns indicating the propensity for organelle sequestration (See Fig. 2, *top row*). Using either fluorescein isothiocyanate- or TRITC-labeled dextran, we have independently confirmed that LTR and QNC colocalize with lysosomes; R123 and R6G were shown to colocalize with fluorescent mitochondrial vital stains Mitotracker Red or Mitotracker Green (representative micrographs are shown in Fig. 6 of supplementary data). We have shown previously that treatment of MDR HL-60 cells with Con A, a specific vacuolar V-ATPase inhibitor, causes lysosome pH to increase from 5.2 to 7.10, which results in a decrease in the lysosome-to-cytosol pH differential. When Con A-treated cells are incubated with LTR and QNC, the lysosomal accumulation is significantly disrupted, consistent with the proposed mechanism for lysosomal accumulation of these compounds (Fig. 2, *middle row*). The mitochondrial accumulation of R123 and R6G are not visibly affected by Con A treatment. DNP is an agent that has been shown to specifically disrupt the mitochondrial membrane potential (17). Cells pretreated with DNP had a significantly reduced capacity to sequester R123 and R6G into the mitochondrial compartment, whereas this treatment did not significantly influence the lysosomal sequestration of LTR and QNC. It is important to note that in Con A-treated cells, LTR and QNC are diffusely localized within the cell and are not, by default, taken up into the mitochondrial compartment. Likewise, R123 and R6G did not accumulate into lysosomes even when the mitochondrial membrane potential was disrupted with DNP. Con A and DNP treatments could potentially alter lysosome and mitochondria morphology, respectively, thereby confounding our results. Immunofluorescence staining of the lysosomal membrane protein Lamp-1 confirmed that cells with disrupted pH gradients had lysosomal morphology similar to cells without pH disruption. Similarly, immunofluorescence staining of the mitochondrial membrane protein Hsp 60 confirmed that disruption of mitochondrial membrane potential with DNP did not visibly affect the morphology of mitochondria (see Fig. 7 of supplementary data). Furthermore, we have confirmed that Con A treatment does not result in redistribution of R123 into lysosomes. Likewise, QNC does not redistribute into mitochondria following DNP treatment (see Fig. 8 of supplementary data).

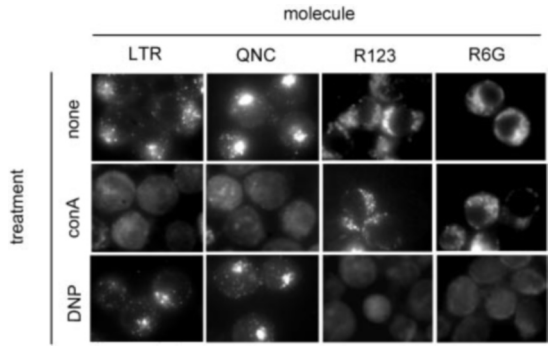

FIG. 2. **The mitochondrial accumulation of R123 and R6G and the lysosomal accumulation of QNC and LTR are driven by independent mechanisms that are not competitive.** The *top row* shows fluorescence micrographs of control (untreated, *none*) MDR HL-60 cells incubated with designated molecules. Both LTR and QNC selectively accumulate with the cell lysosomes, whereas R123 and R6G are sequestered into the mitochondrial compartment of the cell. The cells displayed in the *middle row* have been pretreated with the vacuolar ATPase inhibitor Con A. This treatment disrupts the lysosomal sequestration of LTR and QNC but has no effect on the mitochondrial accumulation of R123 and R6G. The cells displayed in the *bottom row* have been pretreated with DNP, which selectively disrupts mitochondrial membrane potential. Under these conditions, mitochondrial sequestration of R123 and R6G is prevented, whereas this treatment has no effect on the lysosomal sequestration of LTR and QNC.

Together these data confirm the role of membrane potential in the mitochondrial sequestration of R123 and R6G as well as the lysosome-to-cytosol pH differential in the lysosomal sequestration of LTR and QNC. More importantly, these data suggest that the sequestration mechanisms are independent of one another and are not competitive events in the time frame of experimental observation.

The Role of Weak Base Permeability Characteristics—Weakly basic compounds can exist in the un-ionized or ionized form depending on the pH of their environment and the pK_a of the basic functionality. It is routinely thought that ionized compounds have reduced permeability across lipid bilayers relative to un-ionized compounds. The fact that mitochondrial accumulating compounds failed to be sequestered into lysosomes in the presence of DNP led us to consider the possibility that these compounds had unusual permeability characteristics. To assess this behavior, we determined the octanol/water partition coefficient as a function of pH for the compounds shown in Fig. 1. Those compounds with the propensity for lysosomal accumulation (QNC and LTR) showed a typical profile for a weak base. A representative profile from this class of compounds is shown in Fig. 3 (see *QNC plot*). For these molecules, the ionized base (when pH $<$ pK_a) has a significantly reduced partition coefficient relative to the un-ionized base (when pH $>$ pK_a). In striking contrast, those compounds with the propensity to accumulate into mitochondria (R123 and R6G) had pH-independent partitioning behavior (See Fig. 3, *R123* for a representative profile). Using these plots we calculated a parameter that was used to quantitatively describe this permeability behavior. The ratio of the permeabilities of the ionized form relative to the un-ionized form was extrapolated from these plots and was termed α.

The α values for lysosomotropic agents were very low, whereas the values for mitochondrial accumulating compounds were near unity (Table I). Having established this qualitative relationship, we next embarked on establishing a quantitative correlation between α and lysosomal accumulation. Although fluorescence microscopy is a useful approach for observing gross differences in cellular distribution of fluorescent compounds, it is not considered to be quantitative. Therefore we developed a novel approach to quantitate the amount of drug

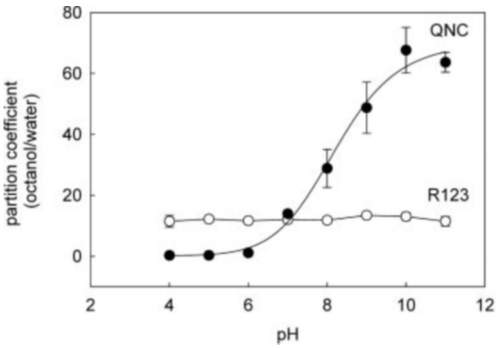

FIG. 3. **Compounds selectively accumulated into the mitochondria of the cells have pH-independent partitioning coefficients. Conversely, compounds accumulating into the lysosomal compartment have typical pH-dependent partitioning coefficients.** A plot of the observed o/w partition coefficient as a function of pH has been compiled for each compound shown in Fig. 1. QNC (*closed circles*) is a representative profile from the class of molecules specifically associated with lysosomes; the *solid line* represents the sigmoidal curve fit to the data. R123 (*open circles*) is a representative profile from compounds specifically accumulated within mitochondria. The ratio of partition coefficients in the ionized form relative to the un-ionized form are extrapolated from these plots and presented in Table I (α). All data points represent the average of three determinations ± S.D.

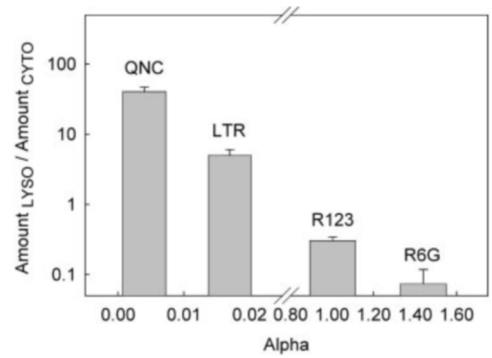

FIG. 4. **Experimentally determined α values correlate with the extent of lysosomal accumulation.** The *bars* represent the amount of each test compound in lysosomes ($Amount_{LYSO}$) normalized to that in cytosol ($Amount_{CYTO}$) plotted against the respective α values. The compounds are identified *above* each bar. The accumulation ratio for each compound is an average of three experiments ± S.D.

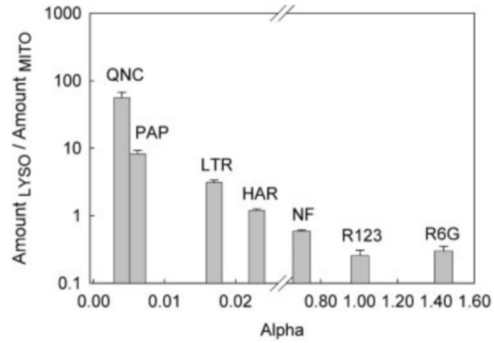

FIG. 5. **Experimentally determined α values correlate with lysosomal *versus* mitochondrial accumulation.** The *bars* represent the ratio of the amount of each test compound in lysosomes ($Amount_{LYSO}$) to that in mitochondria ($Amount_{MITO}$) plotted against the respective α values. The compounds are identified *above* each bar. The accumulation ratio for each compound is an average of three experiments ± S.D.

contained within the lysosomes. This technique utilizes a pulse-chase of cells with FeDex particles. Following the chase period, the endocytosed dextran was specifically accumulated within the lysosomes of cells. The cells were subsequently incubated with drug, homogenized, and passed through a magnetic column that retains lysosomes containing FeDex particles and drug. Drug contained within the lysosomes was then extracted and subsequently analyzed by HPLC. As mentioned earlier, the amount of compound accumulated in lysosomes was normalized to that in cytosol to account for the intrinsic permeability differences between the compounds. Isolation of cell cytosol from MDR HL-60 cells was carried out by a centrifugation procedure developed previously by our laboratory (16). The lysosome-to-cytosol accumulation ratio for each of the fluorescent compounds, previously evaluated qualitatively (Fig. 2), was then plotted against their respective α values. As shown in this plot (Fig. 4), lysosomal accumulation correlated well with experimentally determined α values in an inverse relationship. Furthermore, R123 and R6G failed to achieve significant lysosomal accumulation even after DNP pretreatment, thereby supporting our qualitative results from fluorescence microscopy evaluations (data not shown).

The fact that the high α compounds R123 and R6G preferentially accumulated in the mitochondria (Fig. 2) led us to investigate if the α value of a weak base could be used to predict its lysosomal *versus* mitochondrial accumulation behavior. Our hypothesis was that compounds with low α values (near 0) accumulate predominantly in the lysosomes. Conversely, those compounds high in α values (near 1) accumulate predominantly in the mitochondria. To test this hypothesis, we developed a method to quantitate mitochondrial accumulation of the compounds in MDR HL-60 cells. Isolation of an enriched mitochondrial fraction was accomplished using a differential centrifugation approach. Using enzyme assays, we demonstrated that mitochondrial contamination of the lysosomal fraction was minimal and vice versa (see Fig. 9 of supplementary data). Drug contained within the mitochondrial pellet was extracted and quantitated using HPLC. The ratio of the amount of each compound in the lysosomes to that in the mitochondria was then plotted against the α values of the compounds. A complete listing of calculated α values for compounds evaluated in this study are shown in Table I. These results presented in Fig. 5 demonstrated a good correlation between α and lysosomal *versus* mitochondrial accumulation. Compounds with low α values (*i.e.* QNC) had a higher propensity to accumulate within lysosomes (ratio >1). Conversely, those compounds with high α values (*i.e.* R123) were shown to significantly accumulate within the mitochondrial compartment of the cell (ratio <1). Furthermore, the weak bases PAP, HAR, and NF, with previously undefined intracellular distribution, followed a trend consistent with our hypothesis.

DISCUSSION

We demonstrated here a relationship between a physicochemical parameter of weakly basic compounds and their intracellular localization site. Christian De Duve, credited with the initial discovery of lysosomes, had published a commentary describing the theoretical basis for lysosomal accumulation of weak bases (18). In his work, he speculated that the weak bases with pK_a near neutrality are the best substrates for lysosomal trapping based on a pH partitioning mechanism. Thus, based on our pH measurements in the MDR HL-60 cell line, all of the compounds shown in Fig. 1 are expected to achieve significant lysosomal accumulation. However, delocalized lipophilic cationic compounds, such as R123 and R6G, despite having pK_a near neutrality do not appear to significantly accumulate within the lysosomes of the cell. Alternatively, these compounds preferentially accumulate in the mitochondrial compartment. The driving force for mitochondrial accumulation of these high α compounds is thought to be the negative membrane potential associated with this organelle relative to the

potential existing in the cytosol of the cell. The apparent selective accumulation of R123 and R6G into the mitochondrial compartment with no significant lysosomal sequestration can be rationalized in at least two ways. First, accumulation occurs simultaneously in both compartments with a kinetically favored mitochondrial accumulation. Alternatively, compounds possess physicochemical attributes that make them poor substrates for lysosomal sequestration. Our results favor the latter explanation. In Fig. 2 we show that R123 and R6G fail to appreciably accumulate into lysosomes even in the presence of DNP, a mitochondrial membrane potential-disrupting agent. This result is also supported through quantitative comparisons of the lysosomal accumulation for R123 and R6G with and without DNP pretreatment. Under these conditions, there was no significant change in the extent of lysosomal accumulation (data not shown). As a control, we showed that DNP has no influence on the lysosomal accumulation of LTR and QNC. Our results, which identified R123 and R6G as compounds that failed to accumulate into lysosomes despite the fact that they were both weakly basic and nearly had pK_a neutrality, were intriguing. Attempting to reconcile the basis for the lack of lysosomal sequestration of R123 and R6G, several important factors were considered. First, we reasoned that R123 and R6G should be able to partition into the lumen of the lysosome. This was because the intrinsic permeability values of the un-ionized forms of these compounds were good and comparable with the known lysosomotropic compounds (see Table I, log P values). In fact R6G had a higher log P value than QNC. We also concluded, based upon the experimentally determined pK_a values and lysosomal pH, that these molecules should be >99% ionized when contained within the lumen of lysosomes. From these conclusions, we believe that the difference must be that R123 and R6G can diffuse out of the lysosome in their ionized forms, whereas QNC and LTR cannot. This difference is manifested in the plot of partition coefficient as a function of pH shown in Fig. 3. R123 and R6G have unexpected profiles in which the partition coefficient does not significantly change upon ionization of the molecule. To quantitatively express this characteristic, we extrapolated α values from the profiles represented in Fig. 3. The α value represents a novel physicochemical parameter that has received little previous attention in the literature. We show here for the first time the relevance of this parameter in the biological distribution properties of ionizable weakly basic compounds. Reymond *et al.* (19) have published previously on the influence of charge delocalization on the partition coefficients of ionizable weakly basic compounds. They have demonstrated using cyclic voltametry that charge delocalization results in reduced solvation capacity in aqueous environments. This in turn reduces the free energy of transfer from an aqueous environment to a lipid-like environment, which is manifested by increased octanol-water partition coefficients for delocalized ionized bases. This is in agreement with the results presented in our study. As can be inferred from the structures of compounds in Fig. 1, R123 and R6G have a large degree of delocalization and maintain good membrane permeability even when they exist predominantly in the ionized form. Alternatively, the ionized forms of QNC and LTR have more localized positive charges, which limit their permeability through lysosomal lipid bilayers.

In our quantitative evaluations, we show an inverse correlation between α and the extent of lysosomal accumulation (Fig. 4). In addition, comparison of lysosomal *versus* mitochondrial accumulation (Fig. 5) reveals that an increase in α value not only decreases the extent of lysosomal accumulation but also results in an increase in mitochondrial accumulation. It is noteworthy to mention that a set of weakly basic compounds (PAP, HAR, and NF) with pK_a near neutrality and previously undefined intracellular localization follow a trend consistent with our hypothesis (Fig. 5). Finally, our results suggest that the α value can be used to predict the lysosomal *versus* mitochondrial accumulation tendency. To our knowledge, this work represents the first time that a quantitative approach was successfully used to correlate the physicochemical properties of a compound with its intracellular distribution site.

The findings presented in this manuscript suggest that relatively simple physicochemical measurements can provide a means to evaluate, *a priori*, the propensity for lysosomal *versus* mitochondrial accumulation of weakly basic compounds incubated with cells. Such findings should be extremely valuable for screening compounds obtained from a large library of drug candidates. Likewise, this information can be useful in the theoretical design of drugs with favorable subcellular localization sites and thus improved specificity and activity.

REFERENCES

1. Gottesman, M. M., and Pastan, I. (1993) *Annu. Rev. Biochem.* **62,** 385–427
2. Simon, S., Roy, D., and Schindler, M. (1994) *Proc. Natl. Acad. Sci. U. S. A.* **91,** 1128–1132
3. Gong, Y., Duvvuri, M., and Krise, J. P. (2003) *J. Biol. Chem.* **278,** 50234–50239
4. Hurwitz, S. J., Terashima, M., Mizunuma, N., and Slapak, C. A. (1997) *Blood* **89,** 3745–3754
5. Haugland, R. P. (2002) in *Handbook of Fluorescent Probes and Research Products* (Gregory, J., ed) 9th Ed., p. 483, Moleuclar Probes, Inc., Eugene, OR
6. Skovsgaard, T. (1990) in *Transport and Multidrug Resistance* (Mihich, E., ed) p. 209, John Libbey and Co., New York
7. Moriyama, Y. (1996) *J. Exp. Biol.* **199,** 1447–1454
8. Altan, N., Chen, Y., Schindler, M., and Simon, S. M. (1998) *J. Exp. Med.* **187,** 1583–1598
9. Rottenberg, H. (1979) *Methods Enzymol.* **55,** 547–569
10. Smith, R. A. J., Porteous, C. M., Gane, A. M., and Murphy, M. P. (2003) *Proc. Natl. Acad. Sci. U. S. A.* **100,** 5407–5412
11. Modica-Napolitano, J. S., and Aprille, J. R. (2001) *Adv. Drug Delivery Rev.* **49,** 63–70
12. Binaschi, M., Bigioni, M., Cipollone, A., Rossi, C., Goso, C., Maggi, C. A., Capranico, G., and Animati, F. (2001) *Curr. Med. Chem. Anti-Canc. Agents* **1,** 113–130
13. Rivory, L. P., Avent, K. M., and Pond, S. M. (1996) *Cancer Chemother. Pharmacol.* **38,** 439–445
14. Diettrich, O., Mills, K., Johnson, A. W., Hasilik, A. J., and Winchester, B. G. (1998) *FEBS Lett.* **441,** 369–372
15. Ford, M., Graham, J., and Rickwood, D. (1994) *Anal. Biochem.* **220,** 360–366
16. Duvvuri, M., Feng, W., Mathis, A., and Krise, J. P. (2004) *Pharm. Res.* **21,** 26–32
17. Skulachev, V.P. (1998) *Biochim. Biophys. Acta* **1363,** 100–124
18. De Duve, C., De Barsy, T., Poole, B., Trouet, A., Tulkens, P., and Van Hoof, F. (1974) *Biochem. Pharmacol.* **23,** 2495–2531
19. Reymond, F., Carrupt, P. A., Testa, B., and Girault, H. H. (1999) *Chem. Eur. J.* **5,** 39–47